Supplemental Information

Clinical and functional consequences of *GRIA* variants in patients with neurological diseases

Wenshu XiangWei[1,2], Riley E. Perszyk[2], Nana Liu[1,2], Yuchen Xu[2,a], Subhrajit Bhattacharya[2,b], Gil H. Shaulsky[2,3], Constance Smith-Hicks[4,5], Ali Fatemi[4,5], Andrew Fry[6,7], Kate Chandler[8], Tao Wang[9], Julie Vogt[10], Julie S. Cohen[4,5], Alex R. Paciorkowski[11,], Annapurna Poduri[12,13], Yuehua Zhang[1], Shuang Wang[1], Yuping Wang[14], Qiongxiang Zhai[15], Fang Fang[16], Jie Leng[17,c], Kathryne Garber[18], Scott J. Myers[2,3], Robin-Tobias Jauss[19,20], Kristen L. Park[21], Timothy A. Benke[21], Johannes R. Lemke[19,20], Hongjie Yuan[2,3*], Yuwu Jiang[1*], Stephen F. Traynelis[2,3,22*]

Tables of Contents

Supplemental Table S1: Clinical features and genetic characteristic of patients with *GRIA* variants

See EXCEL file

Supplemental Table S2: Summary of rapid activation, desensitization, and deactivation of GluA4 variant receptors

	WT GluA4	T639S	A643G	A644V
Rise Time (ms)	1.5 ± 0.05	2.9 ± 0.38	4.7 ± 0.23	3.1 ± 0.13
Peak Amp. (pA)	215 ± 14	1419 ± 417	2136 ± 131	502 ± 70
SS Amp. (pA)	8.7 ± 1.1	990 ± 278	1970 ± 122	491 ± 68
SS/Peak (%)	2.2 ± 0.2%	78 ± 4.4%*	92 ± 0.4%*	98 ± 0.6%*
Desensitization: Tau-fast, ms	5.8 ± 0.12	27 ± 1.3	ND	ND
Desensitization: Tau-slow, ms	--	--	ND	ND
Desensitization: % Tau-fast	100%	100%	ND	ND
Desensitization: Tau-weighted, ms	5.8 ± 0.12	27 ± 1.3	ND	ND
Deactivation: Tau-fast, ms	1.3 ± 0.12	6.8 ± 0.4	33 ± 3.0	30 ± 1.8
Deactivation: Tau-slow, ms	7.4 ± 1.1	22 ± 8.9	142 ± 14	247± 16
Deactivation: % Tau-fast	69%	50%	76%	68%
Deactivation: Tau-weighted, ms	5.1 ± 0.82	11 ± 2.8	41 ± 2.3*	94 ± 5.2*
n	14	3	8	5

Whole cell current responses were recorded from HEK cells transiently transfected with WT or variant GluA4 cDNA during 100 msec application of 10 mM glutamate, and the 10-90% rise time, peak amplitude, amplitude at steady-state, and time constants describing desensitization are given as mean ± SEM. n is the number of independent HEK cell recordings. ND: not determined

* $p<0.05$, one-way ANOVA, with Dunnett's multiple comparisons tests compared to WT GluA4 (deactivation Tau_W and SS/Peak % were tested).

Supplemental Table S3: Quantified summary of rapid activation and deactivation of GluA3 variant receptors

	Rise Time (ms)	Peak Amplitude (pA)	Tau_{DESENS} (ms)	Tau_{DEACT} (ms)	SS/Peak (%)	N
GluA3	3.29 ± 0.21	53.8 ± 7.2	9.55 ± 0.79	5.20 ± 0.50	6.6 ± 1.1	13-15
M617T	3.21 ± 0.26	62.8 ± 16.0	8.75 ± 0.51	4.73 ± 0.75	2.4 ± 1.5*	7-10
S647F	2.82 ± 0.19	86.3 ± 21.0	8.16 ± 1.45	3.14 ± 0.29*	4.3 ± 1.4	8-12
A653S	4.22 ± 0.35	60.6 ± 12	14.9 ± 2.7	8.60 ± 2.10	6.9 ± 2.4	6
A653T	3.46 ± 0.30	48.9 ± 11.5	10.3 ± 1.5	5.09 ± 0.81	4.7 ± 1.3	7-10
F655S	3.14 ± 0.34	21.3 ± 3.7	7.25 ± 0.42*	3.81 ± 0.43	10.3 ± 5.8	5-7
V658A	3.42 ± 0.36	54.6 ± 8.7	10.7 ± 2.0	6.00 ± 1.26	5.9 ± 1.8	9
R660S	3.39 ± 0.40	55.3 ± 10.7	10.5 ± 0.64	6.49 ± 0.59	7.3 ± 1.7	7-10
M706T	2.30 ± 0.41	54.3 ± 28.7	6.37 ± 2.27	3.58 ± 1.28	1.7 ± 0.8*	3-4
G803E	3.11 ± 0.28	28.8 ± 6.81	9.33 ± 0.91	6.35 ± 1.00	3.6 ± 1.3	10-14
G806S	3.60 ± 0.35	94.0 ± 21.3	7.92 ± 1.09	5.35 ± 0.74	5.0 ± 2.2	7-8
T816I	3.29 ± 0.42	156 ± 52	8.14 ± 1.40	5.54 ± 0.90	3.1 ± 1.9	6

Whole cell current responses were recorded from HEK cells transiently transfected with WT or variant GluA3 during 1 sec and 5 ms application of 10 mM glutamate, and the 10-90% rise time, peak amplitude, amplitude at steady-state, and time constants describing desensitization are given as mean ± SEM. N is the number of independent HEK cell recordings. The 1 sec application of glutamate was used to determine the desensitization tau and the extent of desensitization (SS/Peak) and the 5 ms application of glutamate was used to determine the deactivation tau. Whole cell recordings were performed because the current amplitudes were too low for outside-out patches. Since whole cell recordings lack the sufficient solution exchange time to isolate the deactivation tau, the deactivation time course of the current response was fit with a dual exponential equation with one of the tau values fixed to the tau determined for desensitization, and the other faster tau was reported for deactivation.

* indicates $p<0.05$ for unpaired t-test, with Bonferroni correction (Tau_{DESENS}, Tau_{DEACT} and SS/Peak % were tested).

Supplemental Table S4: Summary of rescue pharmacology for loss-of-function variants

	100 μM CX614	1000 μM Aniracetam	100 μM Cyclothiazide
WT A3	166 ± 16% (4)	99 ± 1.1% (3)	130 ± 7.4% (4)
A3-F655S	239 ± 15% (4)	97 ± 3.0% (4)	223 ± 26% (4)
A3-M706T	192 ± 19% (4)	82 ± 3.1% (4)	282 ± 44% (4)
WT A4	351 ± 19% (6)	104 ± 1.2% (6)	466 ± 120% (3)
A4-R697P	323 ± 14% (6)	95 ± 3.0% (6)	843 ± 168% (4)

The degree of potentiation was normalized to the agonist-evoked current amplitude in the absence of drug using two electrode voltage clamp recordings from *Xenopus* oocytes in the presence of 1000 μM kainic acid at holding potential of -40 to -60 mV. cRNA encoding human stargazin (γ-2) was co-injected with WT and variant GluA3 cRNA. The data was presented as mean ± SEM % of control, with the number of oocytes recorded given in parentheses.

Supplemental Table S5: Rescue pharmacology for gain-of-function variants (single concentration assay)

	30 μM CP465022	10 μM Perampanel	30 μM GYKI52466	30 μM GYKI53655	100 μM NBQX
WT A3	3.4 ± 1.7% (4)	10 ± 3.8% (6)	44 ± 2.6% (4)	14 ± 2.1% (4)	1.4 ± 1.0% (4)
A3-G803E	5.4 ± 2.4% (4)	12 ± 2.8% (4)	43 ± 0.9% (4)	8.5 ± 2.8% (4)	0.9 ± 0.5% (4)
WT A4	4.7 ± 0.9% (4)	14 ± 3.3% (4)	62 ± 1.6% (4)	14 ± 1.0% (4)	1.1 ± 0.4% (4)
A4-T639S	11 ± 4.2% (4)	21 ± 3.5% (4)	92 ± 7.4% (2)	64 ± 6.0% (4)	0.3 ± 0.1% (3)
A4-N641D	4.8 ± 1.6% (4)	39 ± 1.4% (4)	60 ± 1.6% (4)	22 ± 1.7% (4)	0.2 ± 0.1% (3)
A4-A643G	14 ± 3.4% (6)	53 ± 2.5% (4)	96 ± 4.4% (3)	71 ± 3.3% (4)	1.2 ± 0.4% (4)

The current response in the presence of inhibitor was normalized to the agonist-evoked current amplitude by two electrode voltage clamp recordings from *Xenopus* oocytes in the presence of 1000 μM kainic acid at holding potential of -40 to -60 mV. cRNA encoding human stargazin (γ-2) was co-injected with WT and mutant GluA3. The data was presented as mean ± SEM % of control, with the number of oocytes recorded given in parentheses.

Supplemental Table S6: Summary of rescue pharmacology for gain-of-function variants (concentration-response assay)

	CP465022	**Perampanel**
	IC_{50}, µM [95%CI] (n, %)	**IC_{50}, µM [95%CI] (n, %)**
WT A3	0.3 [0.22, 0.38] (6; 94%)	0.5 [0.30, 0.70] (4; 92%)
A3-G803E	0.4 [0.28, 0.52] (6; 98%)	0.7 [0.11, 1.3] (5; 95%)
WT A4	0.3 [0.24, 0.36] (4; 96%)	0.8 [0.1, 1.6] (3; 89%)
A4-R697P	0.5 [0.36, 0.64] (5; 92%)	4.3 [2.7. 5.9] (4; 70%)

The degree of inhibition was normalized to the agonist-evoked current amplitude using two electrode voltage clamp recordings from *Xenopus* oocytes in the presence of 1000 µM kainic acid at holding potential of -40 to -60 mV. cRNA encoding human stargazin (γ-2) was co-injected with WT and mutant GluA3. The data was presented as mean IC_{50} value [± 95% CI determined form log IC_{50}]. The number of oocytes and maximal inhibition in saturating inhibitor are given in parentheses (n; maximal % inhibition). CI indicates the confidence interval.

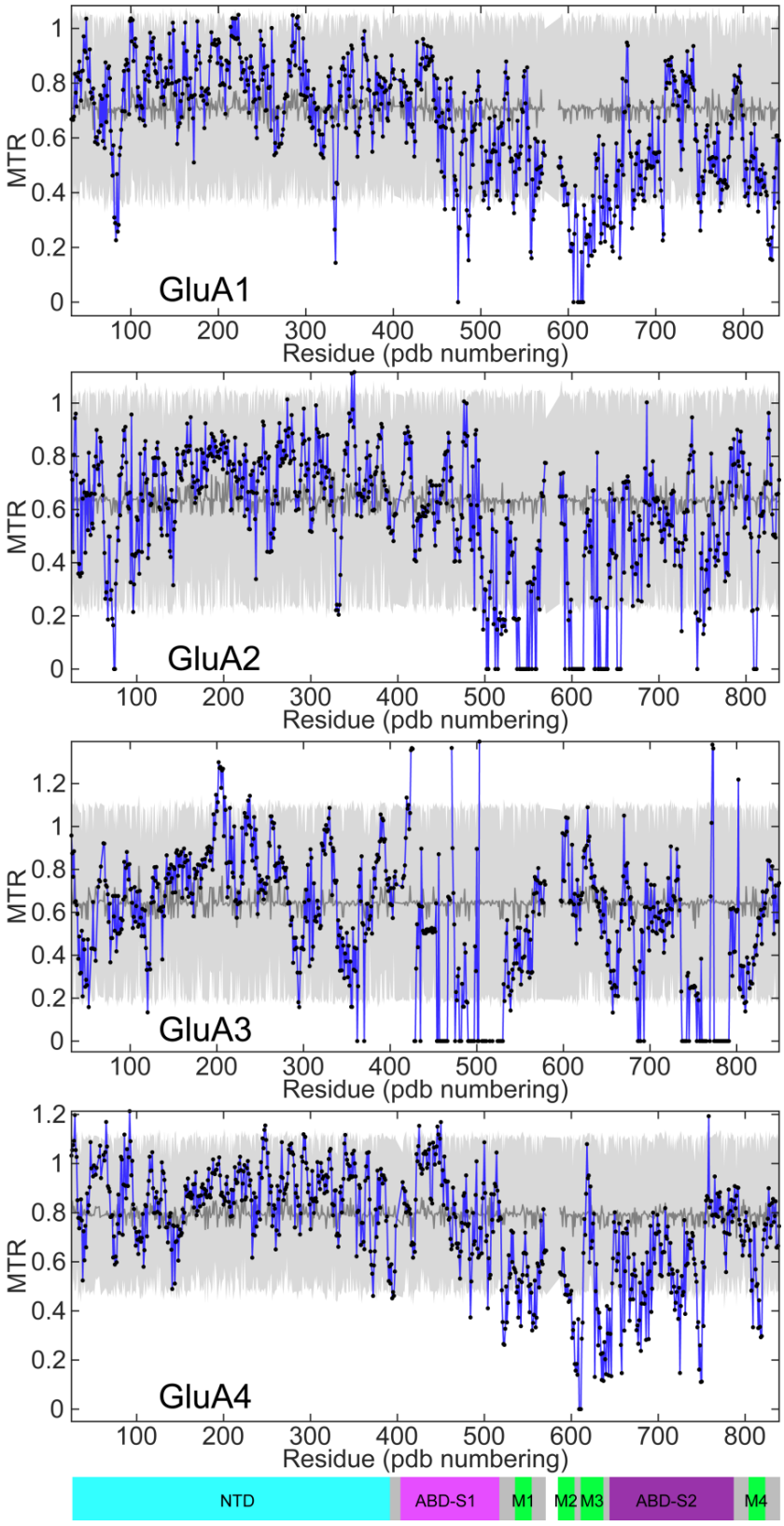

Supplemental Figure S1. 3DMTR scores of homomeric GluA1-4 receptors. The closest 31 residues were used to calculate the intra-receptor 3DMTR (*blue line* and *black dots*, the results for chain A is shown) for *GRIA1*, *GRIA2*, *GRIA3*, and *GRIA4* using the open GluA2 receptor structure. The mean (*grey line*) and 2xSTD range (*grey area*) of the 3DMTR permutation analysis (residue permutation, 1000 instances) are also shown (Perszyk et al. 2020). Note that GluA3 3DMTR score is slightly more volatile due to being X-linked.

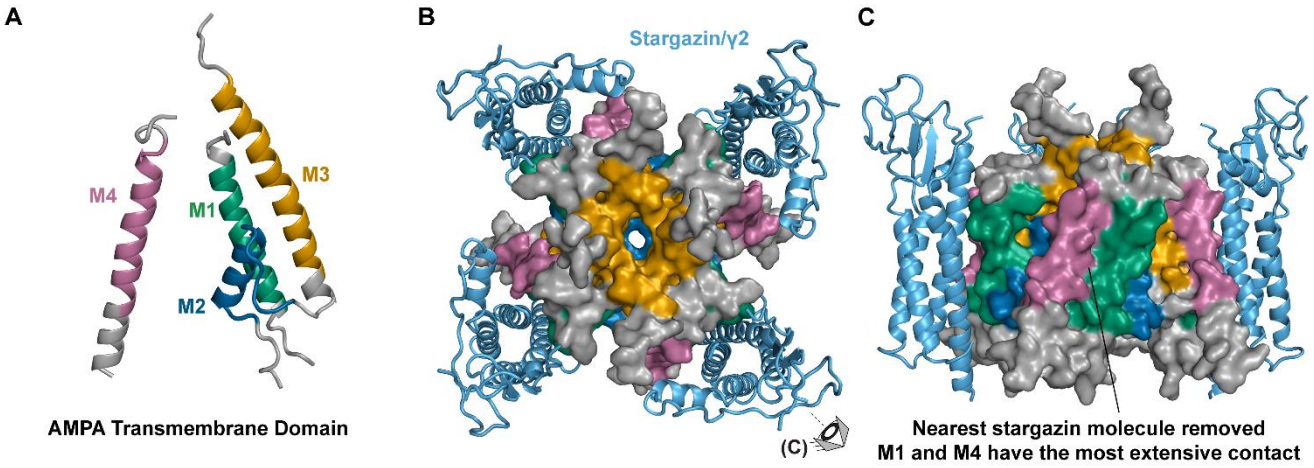

Supplemental Figure S2. Stargazin interacts primarily with the M1 and M4 helices. (***A***) View of the transmembrane domain of a GluA2 subunit (shown in **Figure 2**, PDB:5WEO) shows the inward facing elements. The transmembrane domain helices are differently colored to enhance identification (M1, *green*; M2, *blue*; M3, *orange*; M4, *magenta*). (***B***) Top down view of the GluA2 transmembrane domain. The AMPA receptor subunits are shown as a space-filling model and 4 copies of stargazin are shown in ribbon cartoon (colored cyan). (***C***) Side view of the GluA2 transmembrane domain, as shown in ***B*** with one copy of stargazin removed to highlight the GluA2 transmembrane helices that stargazin interacts with.

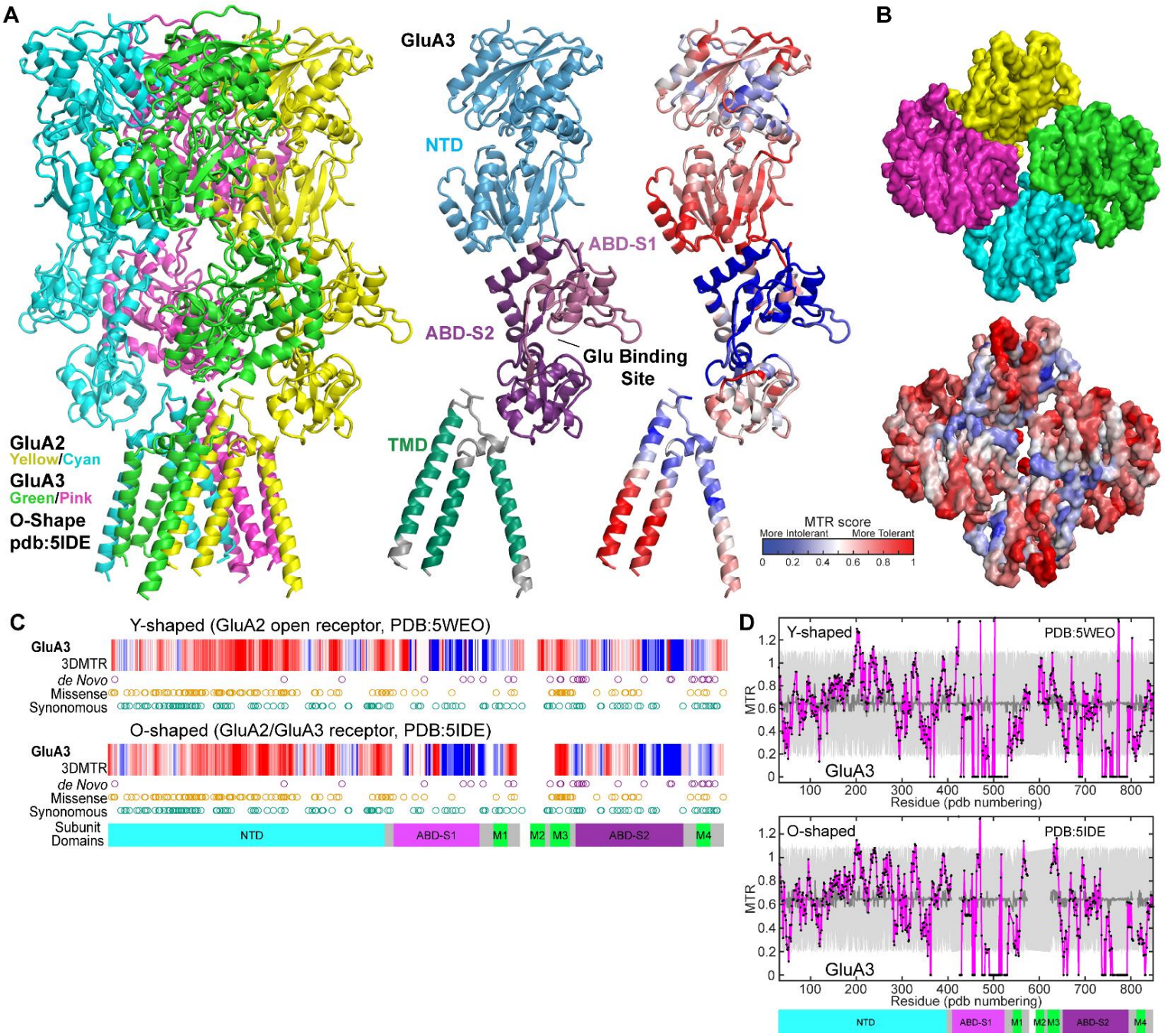

Supplemental Figure S3. Alternative GluA3 3DMTR score based on the O-shaped AMPA structure. (***A***) The ribbon structure of the O-shaped GluA2/GluA3 receptor (PDB:5IDE, Herguedas et al., 2016), including the side view of the tetramer and a view of the isolated chain D showing the semi-autonomous domains (NTD in *blue*, ABD-S1 in *pink*, ABD-S2 in *purple*, and TMD in *green*) and the closest 31 residue intra-receptor 3DMTR. (***B***) Surface of the GluA2/GluA3 NTD structure in the orientation of that in **Figure 4** showing each chain (*top*) and the 3DMTR (*bottom*). (***C***) Linear raster plots of *GRIA3* residues (present in the structure used) depicting the 3DMTR calculated using the Y-shaped structure **Figures 2-4** and the O-shaped structure shown here. The *de novo* variants (*purple*), gnomAD missense variants (*orange*), and gnomAD synonymous variants (*green*) are shown. (***D***) The closest 31 residue intra-receptor 3DMTR (*pink line* and *black dots*) of *GRIA3* using the open GluA2 receptor (*top*) and the O-shaped structure (*bottom*). The mean (*grey line*) and 2xSTD range (*grey area*) of the 3DMTR permutation analysis are shown. Some data are replicated from ***Figure 2*** and included here for clarity.

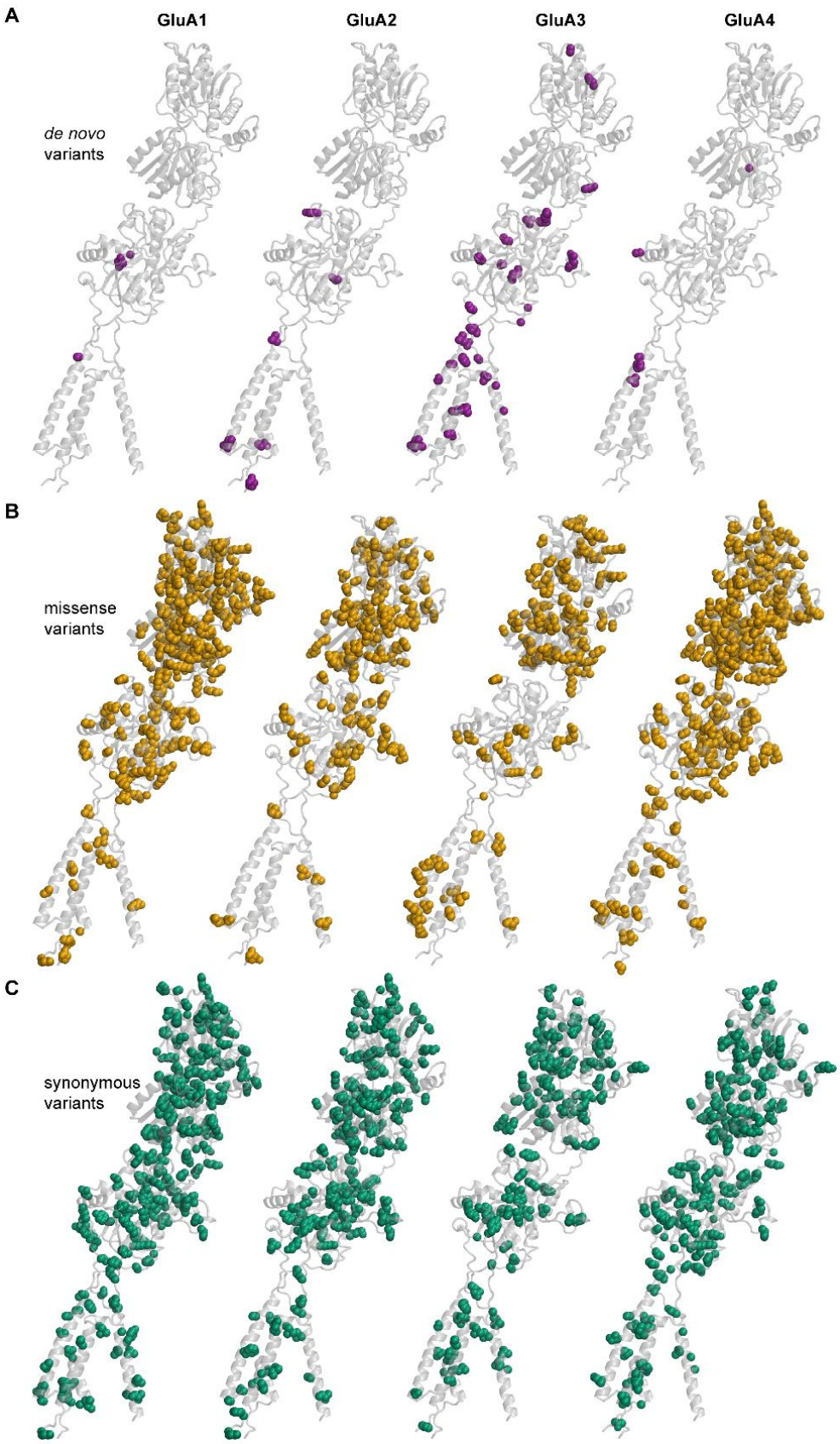

Supplemental Figure S4. Location of *de novo*, missense, and synonymous variants on each GluA subunit. The *de novo* variants (***A***, *purple*), gnomAD missense variants (***B***, *gold*), and gnomAD synonymous variants (***C***, *green*) shown in the linear raster plot in *Figure 2C* are shown as spheres on the subunit structure.

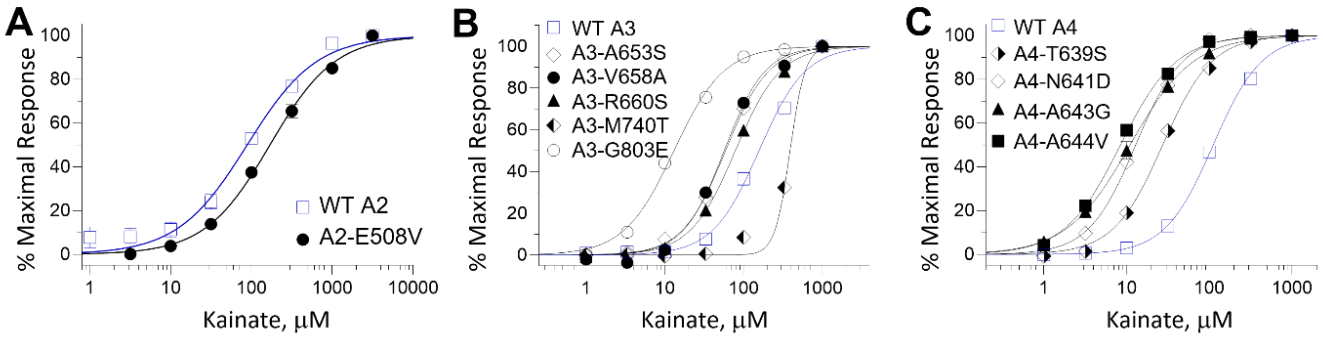

Supplemental Figure S5. The variant GluA2-4 receptors change kainate potency. (***A***-***C***) Composite concentration-response curves for kainic acid recorded at V_{HOLD} -40 mV. Smooth curves are Equation 1 fitted to the data. Data in all composite concentration-response curves are mean ± SEM.

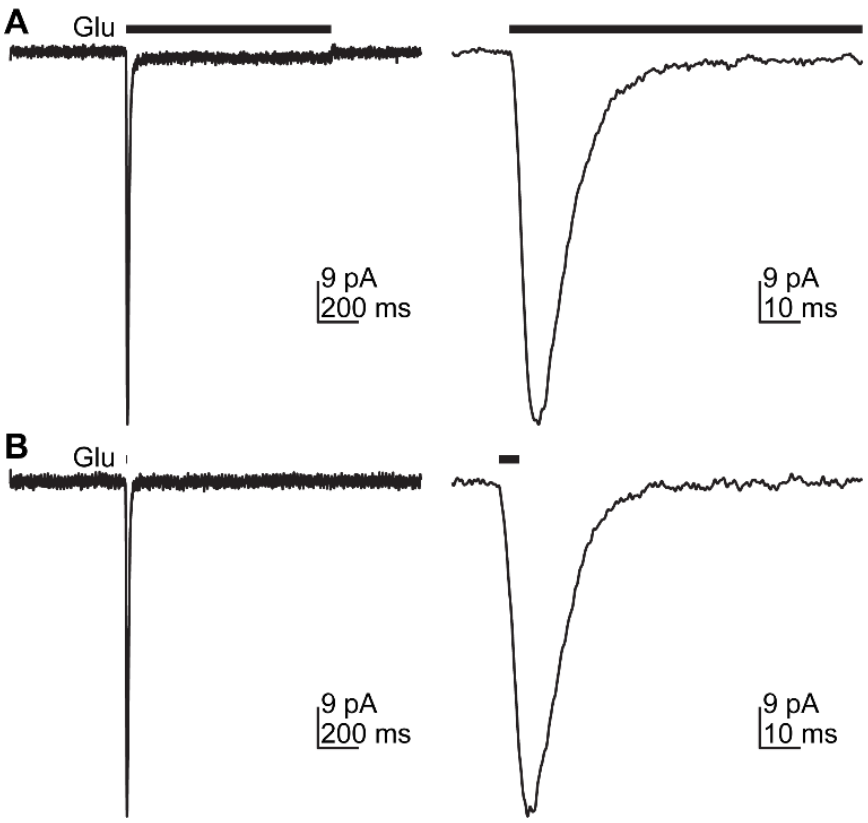

Supplemental Figure S6. Rapid activation and deactivation of GluA3 variant receptors expressed in HEK293 cells. Representative whole cell voltage clamp current recordings are shown in response to application of 10 mM glutamate from WT GluA3 plus human stargazin transfected HEK293 cells. Both long (1 second, ***A***) and short (5 millisecond, ***B***) protocols were performed to determine receptor desensitization and deactivation, respectively. Data describing the time course of the response for WT and variants tested (those with significantly different glutamate EC_{50}, shown in *Table 2*) are shown in *Supplemental Table S2*.

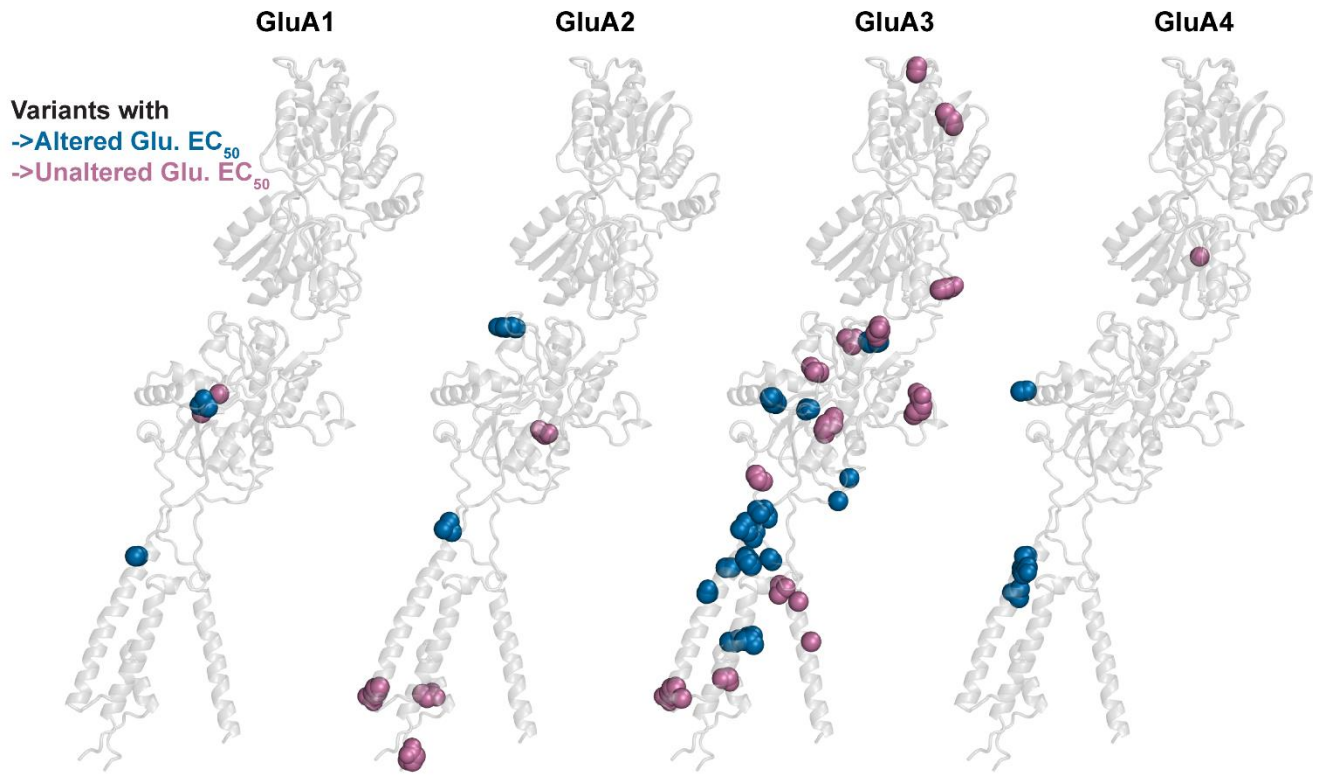

Supplemental Figure S7. Location of tested *GRIA* variants that have altered and unaltered glutamate EC_{50}. The *de novo* variants with altered (*blue*) and unaltered (*magenta*) glutamate EC_{50} determined via TEVC of receptors expressed in *Xenopus laevis* oocytes. If expression prohibited EC50 determination then the variant residue was colored as unaltered (magenta)